Deposition and Characterization of Diamond-like Carbon Films by Electron Cyclotron Resonance Microwave Plasma Enhanced Unbalanced Magnetron Sputtering

Xin Li*, Hui Miao, Hongping Zhu

Shenyang University of Technology, Shenyang 110870, China
lixin97@163.com

We introduce the structure and operational principles of an electron cyclotron resonance microwave enhanced plasma source ion implantation/deposition system for the creation of diamond-like carbon (DLC) film. Using an unbalanced magnetron sputtering process, DLC film was deposited on the silicon substrate using high-purity graphite as the carbon source and argon as the sputtering gas. We used Raman spectroscopy, X-ray photoelectron spectroscopy, and atomic force microscopy characterization methods to study the structure and chemical ratio of the film under different deposition parameters. The results show that the optimal substrate bias and target-substrate distance are 50 V and 150 mm, respectively; when the deposition bias is increased, the film can be made denser and smoother. We also discuss the formation mechanism of DLC film based on the results of structural characterization.

1. Introduction

Diamond-like carbon (DLC) is a metastable form of amorphous carbon containing a significant fraction of sp^3 bonds (Lin et al., 2017). DLC films have been shown to provide a number of useful mechanical properties, including high hardness, low friction coefficient (Zhang et al., 2016), low wear rate and environmental stability (Habibi et al., 2017). Therefore, DLC films are ideal candidates for protective coatings in many applications, such as magnetic storage disks, optical components, metalworking tools, and micro-electromechanical systems (MEMS) (Mahmud et al., 2015). DLC films are prepared by various techniques, such as ion beam deposition, magnetron sputtering, pulsed laser deposition, and radio frequency chemical vapor deposition (Yamamoto et al., 1993). Each technique has its advantages for certain applications. Microwave discharge, especially electron cyclotron resonance (ECR) plasma, develops excellent properties of high degree of ionization and high ions densities. These make ECR microwave plasmas very attractive as a plasma process. In this study, an ECR microwave plasma enhanced source ion implantation/deposition apparatus was applied to prepare the DLC films.

2. Structure and working principle of equipment

Figure 1 shows the equipment needed for our method. Label 1 is the equipment control box. Label 2 is the microwave source with output continuously adjustable between 0 and 1500 W. Label 3 is a square waveguide. Label 4 is an ECR resonant cavity surrounded by an annular water-cooled coil. Two such resonant cavities were symmetrically placed left and right. Label 5 is the ECR resonant cavity power supply. Label 6 is the main vacuum chamber. Label 7 is the triple-stud tuner used to match the impedance between the load and the microwave source.

The main vacuum chamber is cylindrical, with a diameter of 80 cm and a length of 80 cm. The vacuum source uses a mechanical pump and a molecular pump. The stage can be rotated and passed through cooling water. A mass flow meter controls the flow of gas to the ECR resonant cavity. The microwave system uses a 2.45GHz microwave generator, a circulator, a two-way coupler, a triple pin adapter, and a waveguide. The coil's magnetic field produces a magnetic field of 8.75×10^{-2} T.
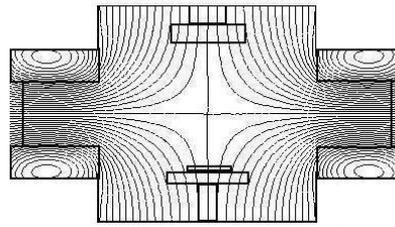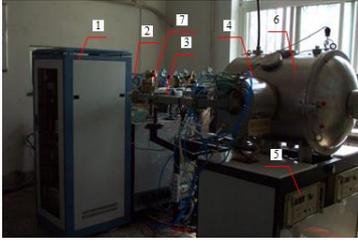
Figure 1: View of MW-ECR-PSII equipment   Figure 2: Radial magnetic field configuration (magnetic line)

At this magnetic field strength, the microwave frequency is the same as the resonance frequency of electrons in the magnetic field, energizing electrons in the resonant cavity via cyclotron resonance. The ions collide with the neutral gas atoms and molecules to generate high-density plasma. By adjusting the size and direction of the excitation coil current, the magnetic field generated by the magnetic coils of the two ECR resonant cavities can be adjusted to form a tangential magnetic field potential type in the main vacuum chamber, as shown in Figure 2. This generated magnetic field and the magnetic field of the magnetically controlled target are superimposed with each other. The result is that that the magnetic field on the surface of the target is no longer closed, and a large magnetic field component perpendicular to the target surface.

The plasma generated by the target discharge is not strongly confined in the vicinity of the sputtering target. Thus, some plasma travels to the surface of the substrate by collision diffusion and the magnetic pressure field, greatly increasing the ion flux density reaching the substrate and causing unbalanced magnetron sputtering. Adjustments to the sputtering and substrate biases change the energy and flux of the sputtering ions reaching the surface of the film, respectively. The height of the stage is adjustable, allowing changes in the distance between the sputtering target and the stage.

3. Experimental methods

We used high-purity graphite as the carbon source with argon as the sputtering gas. After sputter cleaning, we heated the substrate to 100°C and set the ECR magnetic field coil current to 50 A. These conditions placed the ECR resonant plane at the outlet of the discharge chamber, maximizing the plasma density of the deposition chamber. After opening the microwave source, the glow generated by the argon plasma was visible through the observation window. We applied the sputtering bias to clean the target for about 5 s. We applied the deposition bias and opened the baffle to begin the thin film deposition. After 30 min, stopped the deposition. We closed the baffle plate, turned off the sputtering bias, deposition bias, and microwave source, shut down the ECR magnetic field and heating current, and closed the gas source. After natural cooling, released the vacuum and removed the sample. Table 1 shows the parameters for preparation process.

Table 1 Preparation conditions of the DLC film by UMS

Sample	Working pressure (Pa)	Sputtering bias (V)	Deposition bias (V)	Deposition temperature (°C)	Target-substrate distance (mm)
MS-01	0.09	−300	0	300	150
MS-02	0.09	−300	−20	300	150
MS-03	0.09	−300	−50	300	150
MS-04	0.09	−300	−100	300	150
MS-05	0.09	−300	−50	300	200
MS-06	0.09	−300	−50	300	100

4. Results and discussion

Films prepared by different methods have very different structures and properties. We characterized the resulting film from our process qualitatively by visible Raman spectroscopy and X-ray photoelectron spectroscopy. Our prepared film had a high resistivity and was very smooth, such that its surface morphology was not observable with a conventional scanning electron microscope. We had to use an atomic force microscope for this characterization.

4.1 Raman spectroscopy characterization

When the electron cloud is under the action of an electric field, if the deformation in the horizontal direction of the bond is greater than the deformation in the vertical direction, the induced dipole moment changes, and Raman spectrum activity appears. Raman scattering bands that are directly related to sp^3 cannot be observed

by visible Raman spectra excited by 633nm, 514.5nm, or 458nm wavelength light sources. This is because the carbon scattering cross-section of the sp^2 structure is larger than the carbon scattering cross-section of the sp^3 structure. At the same time, the visible light energy is insufficient to stimulate the electrons in the σ state of the sp^3 hybrid orbital, so that visible light of the above three wavelengths can only characterize the Raman scattering effect of sp^2 carbon. However, other research indicates that visible Raman spectroscopy is feasible for qualitative characterization of DLC films (Shi and Sun, 2001).

We took measurements at room temperature using a Renishaw 2000 confocal Raman spectrometer. The laser light source was an argon ion laser with a wave length of 514.5nm, a laser power of 10mW–200mW, a wave number resolution of 2 cm^{-1}, and a scanning range of 200cm^{-1}-2000cm^{-1}.
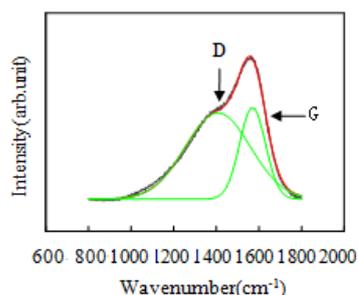

Figure 3: Raman spectrum of MS-03 specimen

Figure 3 shows the Raman spectrum of our film. It is characterized by the presence of a broad scattering peak from 1100 cm^{-1} to 1700 cm^{-1}, which is typical of these carbon films in Raman spectroscopy (Dilou et al., 1984). Two peaks are obtained by fitting the Raman spectral data to a peak splitting process. The low peak wave is called the D peak, and the high wave number is called the G peak. The D peak is a feature shared by disordered carbons. Common belief is that the disorder originates from the disordered bond angles in the microdomains in sp^2 type graphite caused by sp^3-bonded carbon atoms or, alternatively, that it originates due to limited graphite crystallites, whose width is related to sp^2 cluster size. The highly oriented crystalline graphite consists of sp^2 bonds in a planar triangular structure with a first-order Raman spectrum showing the single sharp peak at 1580 cm^{-1}. The G peak is considered to be the downward shift of the peak at 1580 cm^{-1}, corresponding to the stretching vibration mode of C-C bonds (Carlo, 2003).

Overall, Raman spectroscopy qualitatively shows that the film prepared in the test is a diamond-like carbon film. We calculated the area integrals of the D and G peaks to obtain the corresponding peak intensities, I_D and I_G. Shi and Sun (2001) believe that the ratio of the intensity of the D and G peaks (I_D/I_G) is proportional to the ratio of sp^2 and sp^3 bonds in the film. The smaller the I_D/I_G value is, the lower the G-wave direction is toward the lower wave number, and the higher the sp^3 bond content in the film.

Figure 4 shows Raman spectra of films prepared under different bias voltages of the substrate. With a bias voltage of 50 V, the I_D/I_G value was the smallest, and the G peak was at the low wave number, indicating that the sp^3 bond content was maximum at this time. Only when the auxiliary bombardment energy is sufficient to destroy the sp^2 bond with its lower binding energy but not enough to destroy the sp^3 bond with its higher binding energy can the higher sp^3 bond content be obtained. In addition, when the assisted bombardment energy was moderate, the atomic mobility of the film surface was enhanced by ion bombardment, which also facilitated the formation of sp^3 bonds. However, when the bias voltage was too high, the ion energy was very high. After entering the surface layer, the ions retained sufficient energy to diffuse back to the film surface, resulting in a decrease in the nucleation density. When the substrate bias exceeded 200 V, no film could be produced. According to the steady state sheath theory, the bias voltage applied to the substrate mainly fell on the sheath. Therefore, when the deposition bias increased, the ion current density and ion energy also increased. If the energy was too high, re-sputtering of the growth film surface would occur, which was not conducive to the preparation of the film.At target-base distances of 100 mm, 150 mm, and 200 mm, I_D/I_G values were 2.5, 2.3, and 2.6, respectively. A target-base distance of 150 mm produced a higher sp^3 bond content. When the target-base distance was small, the ion energy and density were high, with constant bombardment by high-energy particles, which promoted the transition of some metastable sp^3 bonds to sp^2 bonds. When the target-base distance was large, the ion energy and density were low, resulting in a decrease in sp^3 bond content. When the target-base distance was 50 mm or 250 mm, the film could not be produced. At a target-base distance of 50 mm, the substrate entered the negative glow region. The confinement of the cross field led to the presence of a large number of secondary electrons and ions that caused enough

interactions to prevent film formation. When the target-base distance was too large, the ion density and energy at the surface of the substrate were too low to form a film.
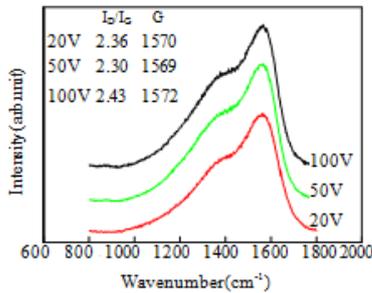

Figure 4: Raman spectra of DLC films under different bias

4.2 X-ray photoelectron spectroscopy (XPS) characterization

The XPS peak position (electron binding energy) gives the chemical state information for the atoms in the thin film. Shifts in the peak position reflect the chemical shifts of the atoms related to the distribution of atoms in the lattice Therefore, XPS is often used to quantitatively analyze sp^3 C content in diamond-like carbon films.
For our XPS analysis, we used an aluminum-magnesium dual anode target with an energy resolution of 0.8 eV, a sensitivity of 80 KCPS, an angular resolution of 45°, and an analysis chamber vacuum of 2.9×10^{-7} Pa. For the sputtering, we used a scanning argon gun with an area of 8×8 mm, a sputtering rate of about 4 nm/min, energy of 3.0 KV, and emission current of 25 mA.
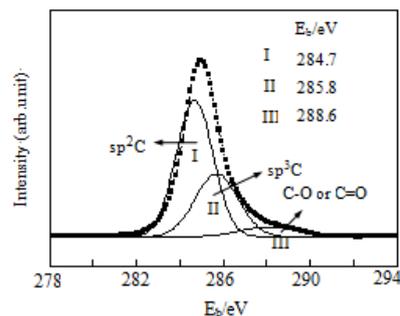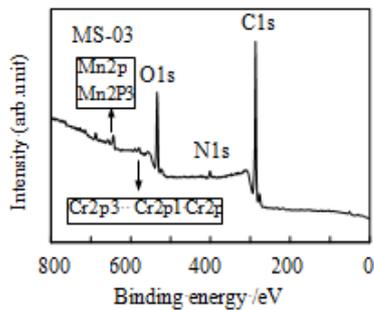

Figure 5: XPS spectrum of the DLC film specimen   Figure 6: C1s spectrum of the DLC film

Figure 5 shows the XPS full spectrum of our samples. The film was mainly composed of carbon atoms and some oxygen atoms. The occurrence of the O1s peak was likely due to the physical adsorption of oxygen on the surface of the sample. There were other elements found in the XPS analysis films, mainly due to argon ions sputtering the base of the magnetic-controlled target. Because of the shape of the peak of our samples, we used the Gaussian curve equation to conduct the spectrum analysis.
Figure 6 shows the C1s electron binding energy spectrum of the film sample. The C1s spectrum of the thin film is divided into three peaks. One occurs where the binding energy is about 284.7eV, which corresponds to the binding energy of sp^2C. Another occurs where the binding energy is about 285.8eV, which corresponds to the sp^3C binding energy. One other occurs where the binding energy is around 288.6eV, which is the binding energy of C-O bond or C=O bond in the film. We integrated the three peaks to calculate the area occupied by each peak. The ratio of the area can be used to evaluate the C ratio of different chemical binding states in the film (Johnston et al., 1994). The content of sp^3C in the DLC film was 32.3% according to MS-03.

4.3 Surface morphology of DLC film

We used a NanoScope IIIA, with a selective scanning range of 1×1 μm^2, for the surface characterization of our films. Figure 7 shows the surface morphology of the films prepared with different substrate biases. As the bias voltage increased, the DLC film gradually became smooth. When the deposition bias was 20 V, the root mean square (RMS) surface roughness of the film was 1.072 nm. Increasing the deposition bias to 100 V produced

a roughness of 0.662 nm. These results show that in our deposition process, the plasma density near the surface of the film growth is high causing the ions to bombard the film surface under the sheath voltage drop effect. This bombardment effect improves the microstructure of the film, producing denser, smoother film. We measured the thickness of our film to be approximately 400 nm.
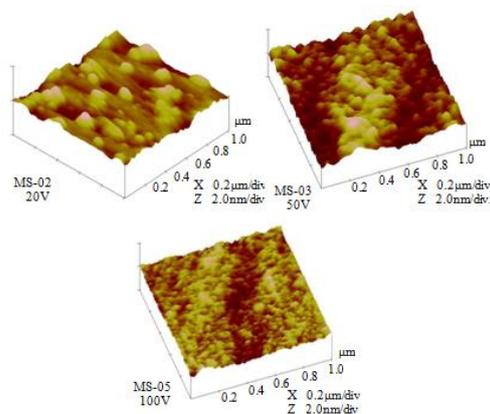

Figure 7: Surface morphology of DLC films under different bias

4.4 Formation mechanism of DLC film

For the mechanism of DLC film formation using PVD, Robertson J. (Robertson, 2002) proposed the subplantation model. Figure 8 shows that when C^+ ions with a certain amount of energy are incident on the surface, they penetrate several atomic layers and enter the subsurface, increasing the density and stress around their location and further resulting in the transition of stable sp^2 bonds to metastable sp^3 bonds at room temperature and pressure. Low energy ions cannot penetrate and remain on the surface of the material to form a stable sp^2 structure. A variety of data and simulation analyses have confirmed the basic concept of the "shallow implantation" model.
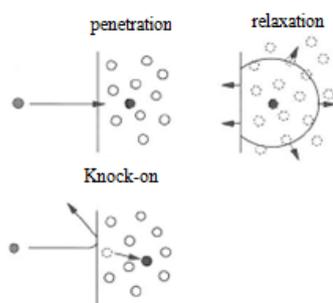

Figure 8: Schematic of the basic processes in subplantation

However, further investigation is needed to explain why high ion energy and deposition temperature suppresses changes in sp^3. From the Raman characterization results of our own process, the sp^3 bond content increased when the substrate bias increased from 20 V to 50 V. When the bias voltage was 20 V, the low ion energy did not readily result in shallow implantation, but the ions only stayed on the growth surface of the film to form a stable sp^2 structure. When the bias voltage was increased to 50 V, more C^+ ions penetrated several atomic layers into the subsurface, thereby forming metastable sp^3 bond content. This also showed that our mechanism conforms to the shallow implantation model. Mckenzie D.R. (Mckenzie, 1993) pointed out that sp^2 bonded graphite has approximately 50% more volume than sp^3 bonded diamonds with the same number of C atoms. Figure 9 shows the phase diagram of diamond and graphite. The diamond phase is stable at the higher pressure part of the Berman Simon line. Robertson J (Robertson, 2002) believed that the particle beam generates a compressive stress in the film, which makes the sp^3 phase of the film rise along the Berman Simon line and stabilize in the high-pressure region. Ions of higher energy may pass through the surface into atomic vacancies or interstitial spaces of the inner surface, thereby increasing the local density and compressive stress of the region where they are located and facilitating the recombination of local bond types

according to the new density. Assuming that the high energy state of ion bombardment exists during the growth of the thin film, the hybridization of atoms can adjust the local density because they are amorphous.
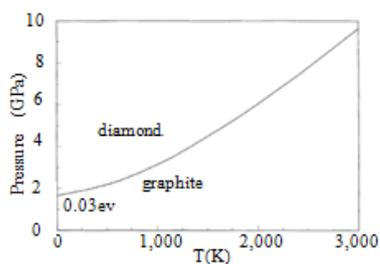

Figure 9: Berman-Simon phase diagram for carbon

5. Conclusions

A diamond-like carbon film was successfully prepared on a silicon substrate using a microwave-electron cyclotron resonance-plasma source ion implantation/deposition system. Raman spectroscopy showed that the film has the characteristics of a typical diamond-like carbon film. XPS characterization results further verified the diamond-like properties of the film. A moderate substrate bias (50 V) favored the formation of sp^3 bonds, and 150 mm was a suitable target-substrate distance. As the substrate bias increased, the diamond-like carbon film gradually became smooth.

Acknowledgments

References

Carlo F., 2003, Deposition and characterization of amorphous carbon nitride thin films, Diamond and related materials, 14, 1154-1163, DOI: 10.1016/0925-9635(94)05282-4

Dilou R.O., Woollam J A, Katkanant V., 1984, Deposition of α-C H films in a Hall accelerator plasma. Phys. Rev., 5, 3482-3487, DOI: 10.1016/0925-9635(94)05204-2

Habibi, S.M. Mousavi K., 2017, Raman spectroscopy of thin DLC film deposited by plasma electrolysis process, Surface & Coatings Technology, 309, 945–950, DOI: 10.1016/j.surfcoat.2016.10.056

Johnston G.P., Tiwari P., Rej D.J., 1994, Preparation of diamond like carbon films by high-intensity pulsed-ion-beam deposition, Journal of Applied Physics, 76, 5949-5945.

Lin Y., Zia A.W., Zhou Z., Shum P.W., 2017, Development of diamond-like carbon (DLC) coatings with alternate soft and hard multilayer architecture for enhancing wear performance at high contact stress, Surf. Coatings Technol, 320, 7-12.

Mahmud. K A., Kalam M., Masjuki H., 2015, An updated overview of diamond-like carbon coating in tribology, Crit. Rev. Solid State Mater. Sci. 40, 90-118.

Mckenzie D.R., 1993, Generation and applications of compressive stress induced by low energy ion beam bombardment, journal of vacuum science & technology, B11, 1928-1035.

Muller U., Hauert R., 1996, XPS investigation of containing diamond-like carbon films, Thin Solid films, 290-292, 323-327.

Robertson J., 2002, Diamond-like amorphous carbon. Materials Science and engineering, R37: 129-281.

Shi J.R., Sun Z., 2001, Resonant raman studies of tetrahedral amorphous carbon films, Diamond and Related Materials, 10, 76-81.

Yamamoto T., Seki K., Takahais M., 1993, Amorphous carbon nitride irradiated with argon ions, Surface and Coatings Technology, 62, 543-547.

Zhang Q., Wang Y., Wang W., 2016, Low voltage and ambient temperature electrodeposition of uniform carbon films, Electrochem. Commun. 63, 22-25.